Prototype of Microwave Imaging System for Breast-Cancer Screening

Rubæk, Tonny; Zhurbenko, Vitaliy

Published in:
Proceedings of ANTEM/URSI 2009

Link to article, DOI:
10.1109/ANTEMURSI.2009.4805106

Publication date:
2009

Document Version
Publisher's PDF, also known as Version of record

Prototype of Microwave Imaging System for Breast-Cancer Screening

Tonny Rubæk and Vitaliy Zhurbenko
Department of Electrical Engineering
Technical University of Denmark
DK-2800 Kgs. Lyngby, Denmark
Email: [tru/vz]@elektro.dtu.dk

***Abstract*—Microwave imaging for breast-cancer detection has received the attention of a large number of research groups in the last decade. In this paper, the imaging system currently being developed at the Technical university of Denmark is presented. This includes a description of the antenna system, the microwave hardware, and the imaging algorithm.**

I. Introduction

An increasing number of research groups are pursuing microwave imaging for biomedical applications, especially breast-cancer detection [1]–[5]. The use of microwave imaging for breast-cancer detection is based on the contrast in electromagnetic parameters between the healthy and the cancerous tissue which has been reported by several authors [6]–[8].

Both nonlinear inverse scattering (also known as microwave tomography) [3], [4], [9] and UWB radar techniques [1], [2], [5] have been proposed for microwave imaging of the breast. When using UWB-based techniques, the resulting images show the point-of-origin of the reflections caused by the tumors while the inverse scattering algorithms reconstruct the spatial distribution of the constitutive electromagnetic parameters, i.e., permittivity and conductivity, of the breast.

At the Technical University of Denmark, a microwave imaging system for breast-cancer screening based on a 3D nonlinear inverse scattering algorithm is currently being developed, and the prototype of this system is described in this paper. The principle of the imaging system is illustrated in Fig. 1. During the examination, the patient is to lie prone atop an examination table with her breast suspended through an aperture in the table. Beneath this aperture, a measurement tank filled with a liquid (glycerin-water mixture) with constitutive parameters close to those of the breast to maximize the coupling of microwave energy to the interior of the breast is positioned. The breast is then irradiated by a single antenna at a time using a single-frequency signal and the response measured on the remaining antennas of the system. By using each antenna in the system as both a transmitter and a receiver, a large number of measurements may be obtained and used as input in an inversion algorithm in which the forward model is based on Maxwell's equations.

This paper is organized as follows: In Section II, the antenna system used in the system is described and in Section III, the microwave hardware which has been developed for performing the measurements is presented. Finally, in Section IV, the imaging algorithm is described.

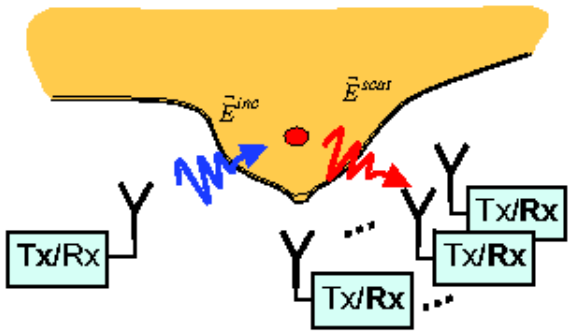

Fig. 1. Imaging principle used in the microwave imaging system. One antenna at a time transmits a sinusoidal signal and the phase and amplitude of the resulting signals are measured by the remaining antennas.

II. Antenna System

A schematic of the antenna system used in the imaging system is shown in Fig. 2. It consists of 32 horizontally oriented monopole antennas positioned in a cylindrical setup with a radius of 8 cm. Although only a single frequency is used in the reconstruction algorithm, the system has been designed for operating at any given frequency in the range from 500 MHz to 3 GHz, thereby allowing for choosing the optimum frequency for the reconstruction.

When designing the antenna setup, three major issues have to be addressed: The first is how to ensure that the imaging system is sensitive to changes in the entire imaging domain, i.e., to ensure that a change in the constitutive parameters of the breast will be detected whether the change is close to the chest wall of the patient or close to the nipple. The second issue concerns the modelling of the field from the antennas: In order to reduce the artifact level in the images, the field used in the imaging algorithm should be identical to the field radiated by the antennas. Any differences will result in an increased artifact level in the reconstructed images. The third and final thing to take into account is the mechanical complexity and

978-1-4244-2980-6/09/$25.00 ©2009 IEEE

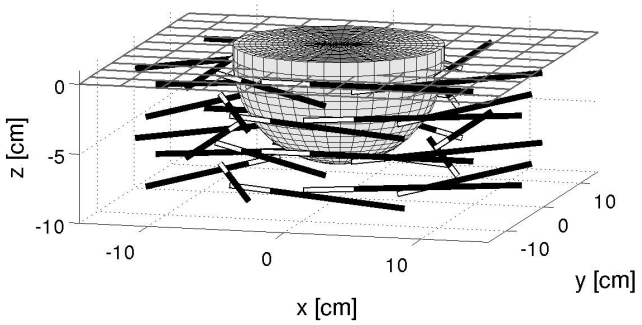

Fig. 2. Schematic of the antenna setup. The antennas are indicated by the black and white lines (white lines indicating the stripped part of the outer conductor). The lid of the measurement tank is indicated by the grid at $z = 0$ cm and the imaging domain is indicated by the light-gray hemisphere.

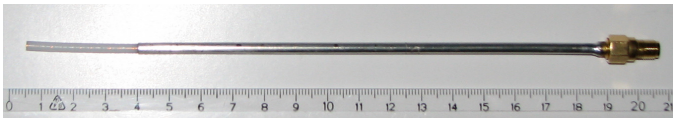

Fig. 3. One of the 32 monopole antennas used in the imaging system.The antenna consists of a coaxial cable from which the outermost 3.5 cm of the outer conductor has been stripped.

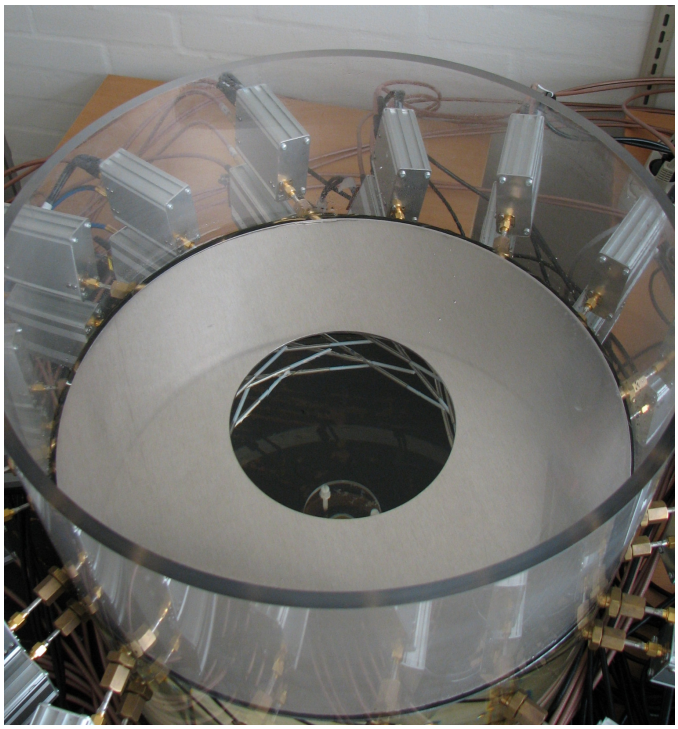

Fig. 4. Photo of the antenna setup used in the imaging system. The monopoles are seen beneath the metallic lid. In the clinical-test system, the measurement tank will be cut off immediately above the metallic lid to allow for the patient to lie prone with her breast suspended through the aperture in the lid.

size of the antennas. Since a large number of antennas must be positioned in a relatively small volume, the antennas must be small and to prevent the antennas from becoming prohibitively expensive to manufacture, as well as to ensure that the 32 antennas are identical, the antennas should be kept simple.

To fulfill these requirements, the design using a cylindrical setup with 32 horizontally oriented monopole antennas has been adapted. A photo of one of the antennas is shown in Fig. 3. This type of antenna was first reported used for microwave imaging in [10] and is easy to manufacture, small in size, and computationally inexpensive to include in numerical models. When inserted in the lossy coupling liquid, the return loss is better than 6 dB throughout the applied frequency range.

The horizontal orientation of the antennas has been chosen to ensure full coverage of the imaging domain. Although a setup using vertically oriented antennas has also been considered due to the increased coupling of the microwave energy between the antennas in such a setup, it has been found that vertically oriented monopoles are less sensitive to changes in the upper part of the imaging domain, close to the chest wall.

A photo of the antenna system mounted in the measurement tank is shown in Fig. 4. The antennas are positioned in a cylindrical measurement tank which is filled with the glycerin-water based coupling liquid mimicking the constitutive parameters of the breast. This liquid is lossy with an effective conductivity of approximately 0.05 - 0.2 S/m in the frequency range used by the system, with increasing conductivity with increasing frequency. Although this is a relatively low loss it is still sufficient to ensure that any signals from the outside of the measurement tank and reflected signals from the wall of the tank are attenuated and hence will not influence the measurements.

At the top of the measurement tank, towards the chest wall of the patient, a metallic lid is used to obtain a known and well-defined boundary. The shielding effect of the metallic lid implies that the measured signals are only affected by that part of the chest wall which is immediately above the aperture. Hence, the imaging domain needs only to be extended slightly into the half space above the lid, as indicated in Fig. 2.

III. Microwave Hardware

Each antenna has been equipped with its own high-sensitivity transceiver module to allow for the large dynamic range required by the system for imaging in the lossy coupling liquid. These transceiver modules are seen as aluminum boxes attached to the antennas in the photo of the antenna setup in Fig. 4.

A schematic of a transceiver modules is shown in Fig. 5. Each module contains a low-noise amplifier (LNA) and a radio frequency (RF) amplifier which amplifies the signal received by the antenna before it reaches the mixer. The local oscillator (LO) generator is operating at a frequency which is offset 1 KHz from the RF frequency and feeds the 32 transceiver modules through a 32-way power divider. After the down conversion, the 1 KHz intermediate frequency (IF) signal is

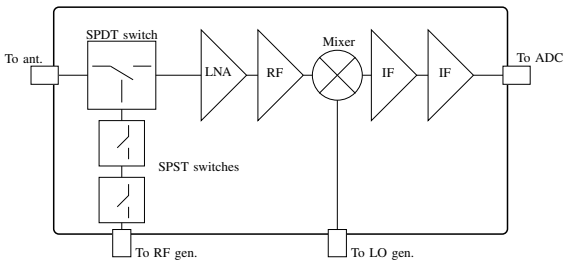

Fig. 5. Schematic of transceiver module. Each transceiver module contains an LNA, an RF amplifier and two IF amplifiers to achieve the necessary dynamic range. The mixer is fed through a power-divider circuitry while the RF generator is connected to the transceiver modules through a switching network which, in combination with the switches in the module itself, minimizes the leakage from the transmitting to the receiving channel.

amplified by two IF amplifiers and fed to an 18 bit analog-to-digital converter (ADC) with a built-in 10 kHz analog low-pass filter.

The digitized signal is processed using a third-order Chebyshev band-pass filter and the amplitude and phase of the resulting sinusoidal signal stored on a computer for later use in the reconstruction algorithm.

The multiplexing between the transmitting and receiving mode of the individual antennas are achieved using a single-pole double-throw (SPDT) switch. However, this switch in itself does not provide sufficient isolation between the signal from the RF generator and the signal from the antenna when this is operating in receive mode. To remedy this, two additional single-pole single-throw (SPST) switches are included in the transceiver modules. Additionally, the RF generator feeds the transceiver modules through a switching network and not a power-divider network as the LO signal.

In addition to the isolation obtained by inserting the additional switches, special attention has been payed to avoid signal leakage within the transceiver modules. This includes filtering of the power supply lines and of the digital lines used for controlling the switches, the use of shielding fences between the receive and transmit blocks in the modules and the use of a minimized PCB enclosure.

The signal which leaks from the SPDT switch to the LNA when a given antenna is acting as transmitter is sampled simultaneously with the signals from the receiving antennas by the ADC. This allows for using the leakage signal as reference when determining the phase of the signals measured by the receiving antennas.

To illustrate the performance of the transceiver modules 1000 measurements of the amplitude and phase of the signal received with an antenna on the opposite side of the imaging domain from the transmitting antenna has been analyzed. During the measurements the system was operating at 2.0 GHz and the measurement tank contained only the coupling liquid, i.e., there were no scattering objects in the imaging system. The 1000 measurements were performed during a time period of approximately 2 hours and 40 minutes since pauses of approximately 10 seconds were inserted between the individual measurements. The ADC was operating with a sampling rate of 100 kHz and used 8000 samples pr. measurement.

The average amplitude of the 1 KHz IF signal measured by the ADC was 0.446 V corresponding to a power level at the terminal of the antenna of approximately -117 dBm. This is 130 dB below the 13 dBm signal which is available from the RF generator and clearly illustrates the need for the very large dynamic range of the microwave hardware. The standard deviation of the 1000 measurements is 5.83 mV, corresponding to 1.3% of the mean amplitude. The mean of the measured phase was 159.57° with a standard deviation of 0.713°. In the preliminary tests, this level of accuracy has been found to be adequate although it may be increased by increasing the number of samples used by the ADC.

The total measurement time (32 transmitters with 31 receivers each) during which the breast of the patient must be suspended through the aperture is approximately 2 minutes pr. breast, including the time needed to fill the measurement tank with the coupling liquid.

IV. Imaging Algorithm

To represent the distribution of the constitutive parameters in the imaging domain, the domain is divided into cubic cells. In each cell, the constitutive parameters are assumed constant and the size of the cells is chosen on the basis of the expected size of the objects to be imaged as well as the wave length in the coupling liquid. Typically, a cube side length of between one tenth and one twentieth of a wave length is used, corresponding to a side length in the order of 2 to 5 mm, depending on the chosen frequency. To represent the permittivity and conductivity of the individual cells, the squared complex wave number is applied. Using the time notation $\mathrm{e}^{i\omega t}$, the squared wave number is given by

$$k^2(\boldsymbol{r}) = \omega^2 \mu_0 \epsilon(\boldsymbol{r}) + i\omega\mu_0\sigma(\boldsymbol{r}) \tag{1}$$

wherein i is the imaginary unit, ω is the angular frequency, and μ_0 is the free-space permeability. The conductivity is given by σ and the permittivity by ϵ with $\boldsymbol{r}$ indicating the position.

A nonlinear inverse-scattering algorithm is applied in the system to reconstruct the three-dimensional distribution of the constitutive electromagnetic parameters in the imaging domain. In this algorithm, the distribution is reconstructed by solving the nonlinear minimization problem

$$\begin{aligned}\underline{k}^2 &= \operatorname{argmin}\left\{\left\|\underline{S}^{\mathrm{meas}} - \underline{S}^{\mathrm{calc}(\underline{k}^2)}\right\|_2^2\right\} \\ &= \operatorname{argmin}\left\{\|\underline{S}^{\mathrm{res}}\|_2^2\right\}\end{aligned} \tag{2}$$

using an iterative Newton algorithm. Herein, the column vector $\underline{S}^{\mathrm{meas}}$ holds the measured data and $\underline{S}^{\mathrm{calc}}$ holds the corresponding data calculated assuming the distribution of squared wave numbers given by $\underline{k}^2$. The column vector $\underline{S}^{\mathrm{res}}$ is the residual vector. The minimization problem is formulated using the log-magnitude and unwrapped phase formulation introduced in [11] which has been shown to improve the performance of the algorithm by emphasizing large relative

changes and allowing for reconstructions to span multiple Riemann sheets.

In each of the N iterations of the Newton algorithm, the following three steps are performed (with n indicating the iteration number):

1) Calculate the signals resulting from the distribution of squared wave numbers given by the column vector $\underline{k}_n^2$ and the corresponding Jacobian matrix J_n. To this end, a method-of-moments code utilizing the adaptive integral method and higher-order basis functions [12] is used.
2) Solve the linear problem

$$\underline{\Delta k}_n^2 = \operatorname{argmin} \left\{ \left\| \underline{\underline{J}}_n \underline{\Delta k}_n^2 - \underline{S}_n^{\mathrm{res}} \right\|_2^2 \right\} \quad \text{subj. to regularization.} \quad (3)$$

to determine the update vector $\underline{\Delta k}_n^2$. This problem is ill-posed in the classical sense and regularization must be applied to achieve a suitable solution. To this end an algorithm using the conjugated gradient least squares algorithm [13, Sec. 6.3] in combination with a trust-region [14], the L-curve criterion [13, Sec. 7.5], and a Euclidean-distance penalty term [15] has been applied.
3) Update the distribution of complex squared wave numbers using

$$\underline{k}_{n+1}^2 = \underline{k}_n^2 + \alpha_n \underline{\Delta k}_n^2 \quad (4)$$

with the scalar α_n being the Newton step [16]. The Newton step is most often unity, although in some circumstances it is less than one to ensure that the phase of the calculated signal is unwrapped properly [4].

The most time-consuming task in the reconstruction is solving the forward problem. This may take as much as 30 minutes to complete, although 15 minutes is more typical for a standard discretization of the imaging domain. After the forward solution $\underline{S}^{\mathrm{calc}}$, and thus $\underline{S}^{\mathrm{res}}$, has been found, the calculation of the Jacobian and the update of the distribution is found in less than half a minute. The reconstruction algorithm typically converges within the first 12 iterations, yielding a total reconstruction time of 3 - 6 hours depending on the time used solving the forward problem.

Preliminary studies have shown that the system is capable of detecting spherical scatterers with a diameter less than 5 mm and a number of reconstructions of phantom measurements will be presented at the conference.

V. Conclusion

A prototype system for microwave imaging of the breast was presented. The system consists of three major parts; an antenna system, a set of microwave transceiver modules and an ADC for storing the measured data, and, finally, a reconstruction algorithm. The antenna system has been designed to achieve a near-uniform coverage of the imaging domain and minimum influence from the surroundings while the transceiver modules has been designed for quick examination with a dynamic range of more than 130 dB. The nonlinear inversion algorithm applies the log-magnitude unwrapped phase formulation to improve its performance as well as a method-of-moments algorithm which has been optimized for use in the reconstruction.

Acknowledgment

This work is supported by the Villum Kann Rasmussen Foundation, grant no. VKR020891.

References

[1] W. C. Khor, *et al.*, "An experimental and theoretical investigation into capabilities of a UWB microwave imaging radar system to detect breast cancer," *EUROCON, 2007. The International Conference on Computer as a Tool*, pp. 771–776, 2007.

[2] M. Klemm, *et al.*, "Experimental and clinical results of breast cancer detection using UWB microwave radar," *Proceedings of the IEEE Antennas and Propagation Society International Symposium, 2008*, 2008.

[3] J. Johnson, T. Takenaka, and T. Tanaka, "Two-dimensional time-domain inverse scattering for quantitative analysis of breast composition," *IEEE Transactions on Biomedical Engineering*, vol. 55, no. 8, pp. 1941–1945, 2008.

[4] T. Rubæk, *et al.*, "Nonlinear microwave imaging for breast-cancer screening using Gauss-Newton's method and the CGLS inversion algorithm," *IEEE Transactions on Antennas and Propagation*, vol. 55, no. 8, pp. 2320–2331, 2007.

[5] T. Williams, J. Sill, and E. Fear, "Breast surface estimation for radar-based breast imaging systems," *IEEE Transactions on Biomedical Engineering*, vol. 55, no. 6, pp. 1678–1686, 2008.

[6] W. T. Joines, *et al.*, "The measured electrical properties of normal and malignant human tissues from 50 to 900 MHz," *Medical Physics*, vol. 21, no. 4, pp. 547–50, 1994.

[7] S. P. Poplack, *et al.*, "Electromagnetic breast imaging: Results of a pilot study in women with abnormal mammograms," *Radiology - Radiological Society of North America*, vol. 243, no. 2, pp. 350–359, 2007.

[8] M. Lazebnik, *et al.*, "A large-scale study of the ultrawideband microwave dielectric properties of normal, benign and malignant breast tissues obtained from cancer surgeries," *Physics in Medicine and Biology*, vol. 52, no. 20, pp. 6093–6115, 2007.

[9] P. Hashemzadeh, *et al.*, "Experimental results of an optimization approach to two-dimensional time domain electromagnetic inverse problem with application to microwave breast tomography," *Proceedings of the 3rd IASTED International Conference on Biomedical Engineering, 2005*, pp. 192–196, 2005.

[10] P. Meaney, *et al.*, "An active microwave imaging system for reconstruction of 2-D electrical property distributions," *IEEE Transactions on Biomedical Engineering*, vol. 42, no. 10, pp. 1017–1026, 1995.

[11] ——, "Microwave image reconstruction utilizing log-magnitude and unwrapped phase to improve high-contrast object recovery," *IEEE Transactions on Medical Imaging*, vol. 20, no. 2, pp. 104–116, 2001.

[12] O. S. Kim and P. Meincke, "Adaptive integral method for higher order method of moments," *IEEE Transactions on Antennas and Propagation*, vol. 56, no. 81, pp. 2298–2305, 2008.

[13] P. C. Hansen, *Rank-Deficient and Discrete Ill-Posed Problems: Numerical Aspects of Linear Inversion*, ser. Monographs on Mathematical Modeling and Computation. SIAM, 1998.

[14] D. C. Sorensen, "Newton's method with a model trust region modification," *SIAM Journal on Numerical Analysis*, vol. 19, no. 2, pp. 409–426, 1982.

[15] D. Li, P. Meaney, and K. Paulsen, "Conformal imaging with a non-contacting microwave antenna array," *Proceedings of the IEEE MTT-S International Microwave Symposium, 2001*, vol. 1, pp. 563–566, 2001.

[16] C. T. Kelley, *Iterative Methods for Linear and Nonlinear Equations*, ser. Frontiers in Applied Mathematics. Philadelphia, PA: SIAM, 1995, vol. 16.